JOURNAL OF THEORETICAL
AND APPLIED MECHANICS
64, 1, pp. 45–56, Warsaw 2026
https://doi.org/10.15632/jtam-pl/214577

EVALUATION OF VISCOSITY AND RHEOLOGICAL CHARACTERISTICS OF CORN OIL COMBINED WITH GRAPHENE NANOPLATELETS FOR MACHINING LUBRICATION

Pungky EKA SETYAWAN, Anindito PURNOWIDODO*, Achmad AS'AD SONIEF, Yudy SURYA IRAWAN

Faculty of Engineering, Universitas Brawijaya, Malang, East Java, Indonesia
*corresponding author, *anindito@ub.ac.id*

This study aims to analyze the thermal conductivity, dynamic viscosity and rheology of corn oil (CO) with added graphene nanoplatelets (GNPs). The addition of GNPs to CO uses variations of $\Phi = 0.10\,\%$, $\Phi = 0.15\,\%$, $\Phi = 0.20\,\%$, $\Phi = 0.25\,\%$, and $\Phi = 0.30\,\%$. The highest thermal conductivity results were produced at a GNP percentage of $\Phi = 0.30\,\%$ with a value of $0.1620\,\mathrm{W \cdot m^{-1} \cdot K^{-1}}$. The viscosity results show that the highest dynamic viscosity value is produced at GNPs $\Phi = 0.20\,\%$ at all temperatures. The rheology results show that the stable percentage $0.10\,\%$ and $0.20\,\%$ approaches Newtonian properties.

Keywords: thermal conductivity; rheology; corn oil; graphene nanoplatelets; cutting fluid.

1. Introduction

Machining is the process of shaping a workpiece by removing material using a cutting tool. The cutting tool rubs against the material, directly generating significant heat. This significant heat can damage or wear the cutting tool components (Da Silva *et al.*, 2011). Therefore, cutting fluids are crucial for lubrication, cooling, and removing cutting material.

Vegetable oil is an alternative fluid for the machining cooling process. The cooling process is more effective because vegetable oils offer advantages such as a thick film, reduced friction, cutting force, cutting tool wear, and heat reduction (Debnath *et al.*, 2014). Research has frequently been conducted on the use of vegetable oils as cutting fluids, including cottonseed oil, coconut oil, soybean oil, canola oil, castor oil, palm oil, and sunflower oil (Gunjal & Patil, 2018).

Several vegetable oils have disadvantages, including castor oil (high viscosity that can impede fluid flow in the cutting zone), coconut oil (limited performance at high temperatures), and sunflower oil (expensive and limited availability). In contrast, corn oil (CO) offers relatively high saturated fatty acids, enabling it to form a strong film, with moderate viscosity, heat stability, and abundant availability. Therefore, based on these superior properties, CO is a prime candidate for base fluid in cutting fluid applications (Arsene *et al.*, 2021).

Improvements to vegetable oils in cutting fluids have been frequently attempted to enhance their properties, one example being the addition of graphene (Samuel *et al.*, 2011). The addition of graphene reduces friction between the cutting tool surface and the workpiece (Park *et al.*, 2011). This friction reduction results in a gradual, linear reduction in cutting force and temperature with increasing graphene percentage (Uysal, 2017). Furthermore, this reduction also depends on the minimum quantity lubrication (MQL) parameters and the proportion of graphene.

Numerous studies have been conducted to improve the performance of cutting fluids using graphene. Wang *et al.* (2022) examined the effect of adding graphene nanoplatelets (GNPs) and a sulfurized additive to an MQL system in the machining process of Ti-6Al-4V titanium alloy. Graphene nanoplatelets were added at concentrations of 0.05 %, 0.10 %, and 0.20 %, then mixed with the sulfurized additive. Test results showed a reduction in the tool wear rate of up to 31 % and a reduction in surface roughness of 18 %. Crystallographic microscopy observations revealed an even distribution of nanoparticles, improving lubrication and cooling capabilities. Overall, this nanofluid was able to extend tool life, improve surface quality, and improve thermal efficiency (Wang *et al.*, 2022). Caglayan (2021) evaluated the rheological and tribological properties of an oil-based nanofluid modified with silylated GNPs. This nanofluid was prepared by dispersing silane-modified graphene sheets into a base oil without the addition of surfactants or dispersants. Tribological tests were conducted using a ball-on-disk universal friction and wear tester. The test results showed that the addition of silylated GNPs significantly improved lubrication properties and wear resistance, with a reduction in the friction coefficient of up to 40 % and a reduction in wear of 35 % compared to pure base oil.

In a study by Bertolini *et al.* (2021), the use of GNPs as an additive in the MQL system while turning Inconel 718 alloy was shown to provide significant benefits. Graphene additives with concentrations of 0.05 % and 0.10 % were added to vegetable oil as a cutting fluid. The goal is to extend the life of the cutting tool by up to 50 % and improve the surface quality of the machined samples compared to using pure vegetable oil. These improvements are explained by a reduced coefficient of friction between the tool and chips, and increased cooling effectiveness in the cutting zone (Bertolini *et al.*, 2021).

Ramón-Raygoza *et al.* (2016) investigated the rheological and tribological characteristics of an oil-based nanofluid enriched with silane-modified GNPs, without the use of surfactants. Characterization was performed using friction force microscopy and phase contrast microscopy. The results showed that the addition of GNPs improved lubrication and wear resistance, with a 43 % reduction in the friction coefficient and a 63 % increase in wear resistance at a 2 % GNP concentration in the engine oil. The development of this nanofluid supports technological innovation for the modern manufacturing industry, focused on sustainable and environmentally friendly practices.

Vora *et al.* (2023) investigated the rheological properties and thermal conductivity of a nanofluid based on graphene nanoplatelets and castor oil. The nanofluid was prepared by mixing GNPs and castor oil, followed by ultrasonication to obtain a stable dispersion. Test results indicate that GNP/castor oil nanofluid exhibits Newtonian flow, with viscosity decreasing with increasing shear rate.

Manikanta *et al.* (2024) examined the combination of GNPs and CO for cooling during turning machining. GNP concentrations varied from 0.50 % to 3 %, with cutting forces and tool wear reduced by 2.5 %. The rheological characteristics of this study were not investigated.

The highly saturated acid content of CO, as compared to other vegetable oils, will affect lubrication efficiency and film strength. However, research related to cutting fluids using CO as a base fluid with added GNPs is still limited. Furthermore, testing has focused only on tool wear or cutting force reduction, but has never comprehensively analyzed rheological properties. While rheological characteristics are generally essential for analyzing fluid flow, heat transfer, and lubrication, this study aims to fill this gap by characterizing the thermal conductivity, dynamic viscosity, and rheological properties of cutting fluids.

2. Experimental procedure

The method used in this study included the preparation of GNPs. The resulting GNPs were then validated by morphological testing using scanning electron microscopy (SEM) and crystal structure using X-ray diffraction (XRD). The GNPs were then mixed with CO as a base

lubricant. The resulting mixture was then analyzed for thermal conductivity, dynamic viscosity, and rheology.

2.1. Preparation of GNPs/nanofluids

This study used CO as the base oil, which was combined with GNPs to form the nanofluid shown in Fig. 1. The preparation of nanofluids requires more attention to achieve a stable liquid suspension without precipitation. The GNPs used were type KNG-150, with a purity of 99 %, a thickness of 5 nm–10 nm, and a width of 10 µm, produced by Knano Nanotechnology Group (KNG), China. Mazola CO was produced by ACH Food Companies, Inc., USA. The properties of CO are shown in Table 1.

Fig. 1. Photo of pure CO nanofluid and nanofluid Φ 0.10 % to Φ 0.30 %.

Table 1. Properties of CO.

Property	Value
Appearance	Bright golden-yellow color
Specific gravity (at 25 °C)	0.92
Hydroxyl value	0.7–1.5
Saponification value	190–195
Iodine value	110–120
Acid (mg KOH/gram of oil)	0.5–2.0

The preparation of nanofluids aims to produce a homogeneous, stable, durable, and minimally sedimented mixture dispersion, as shown in Fig. 2.

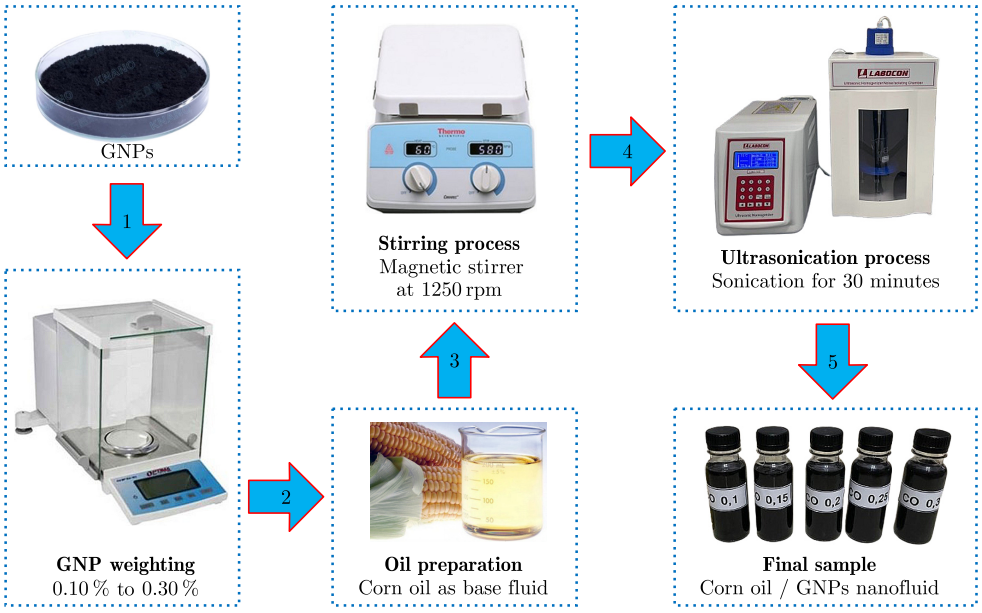

Fig. 2. Schematic of preparation of CO nanofluids combined with GNPs.

The preparation of a mixture of CO and GNP nanofluid was carried out using a two-step method. First, GNPs were weighed accurately using an analytical balance (Optima OPD-E204,

±0.1 mg), with varying concentrations of $\Phi = 0.10\,\%$, $\Phi = 0.15\,\%$, $\Phi = 0.20\,\%$, $\Phi = 0.25\,\%$, and $\Phi = 0.30\,\%$ of the weight of CO. GNPs were added to CO in a beaker, then stirred with a magnetic stirrer at 1250 rpm for 20 min to obtain an initial dispersion. The process was continued with ultrasonic dispersion for 30 min to ensure a stable dispersion and reduce agglomeration of graphene particles.

2.2. Material characterization

The morphology and crystal structure of GNPs were analyzed using SEM and XRD. Figure 3 shows the surface morphology of GNPs, with SEM results at 10 000× and 100 000× magnifications indicating that the GNP nanoparticles have a typical platelet shape, consistent with the GNP datasheet. The crystal structure of GNPs was analyzed using XRD, as shown in Fig. 3. This material characterization is important for identifying material properties, including shape, composition, chemical compounds, and functional groups, in order to understand the material's behavior in specific applications.

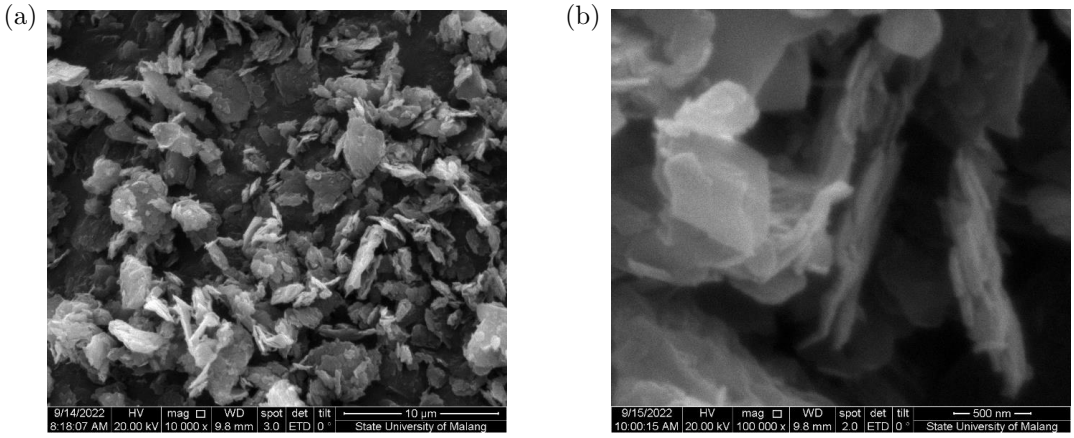

Fig. 3. Results of graphene morphology at magnifications of (a) 10 000× and (b) 100 000×.

XRD testing was conducted to examine the crystal structure and phase of graphene nanomaterials, as shown in Fig. 4. Sharp peaks at $2\theta = 26.4336°$ ((002) plane) and $2\theta = 54.5347°$

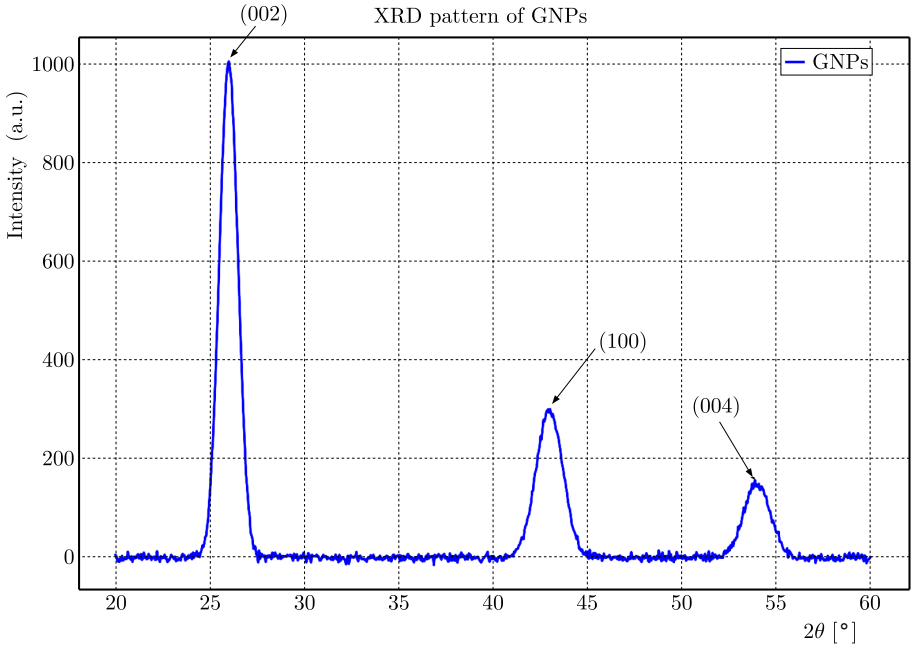

Fig. 4. XRD test graph of graphene nanomaterial.

((004) plane) indicate graphene's typical hexagonal crystal structure. These results indicate that the nanomaterial used is high-quality GNPs. Furthermore, the average crystallite size, calculated using the Scherrer equation, was 31.889 nm at 26.4336° and a FWHM of 0.2558 nm.

2.3. Thermal conductivity

The thermal conductivity of nanofluids was measured with a KD2 Pro Thermal Properties Analyzer using the Modified Transient Plane Source method at a temperature of 30 °C.

2.4. Dynamic viscosity

The dynamic viscosity of nanofluids was measured using an NDJ-8S viscometer at 30 °C and 100 °C. The viscometer geometry used spindles (radius (R_b) = 0.094 cm, cup radius = 0.1405 cm, and length = 0.65 cm). The spindle rotation speeds (n) used were 6 rpm, 12 rpm, 30 rpm, and 60 rpm. The angular velocity was then calculated for each rpm using:

$$\omega = \frac{2\pi}{60} n, \tag{2.1}$$

where ω – angular velocity [rad/s], n – rotation speed [rpm].

From the angular velocity results, the shear rate is then calculated using:

$$\gamma = \frac{2\omega R_{C^2} - R_{b^2}}{x^2(R_{C^2} - R_{b^2})}, \tag{2.2}$$

where γ – shear rate [s^{-1}], ω – angular velocity (spindle) [rad/s], R_C – vessel radius [cm], R_b – radius (spindle) [cm], X – radius at which the shear rate is being calculated [cm].

From the calculation results in Eq. (2.2), the shear rates are 0.0012 s^{-1}, 0.0022 s^{-1}, 0.0055 s^{-1}, and 0.01105 s^{-1}.

3. Results and discussion

3.1. Thermal conductivity

The results of the thermal conductivity test of nanofluids performed with the KD2 Pro Thermal Properties Analyzer are presented in Fig. 5.

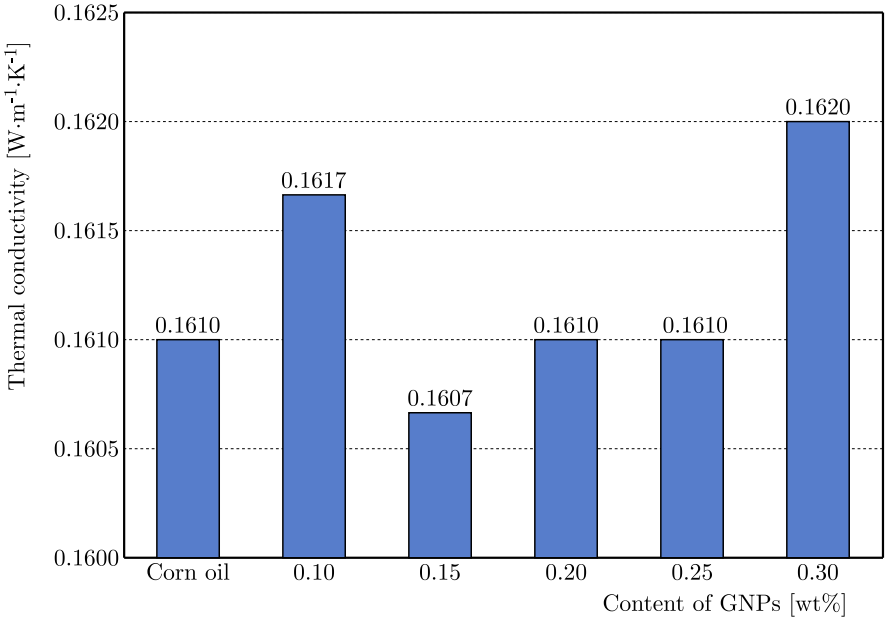

Fig. 5. Thermal conductivity of CO nanofluids with varying concentrations.

Based on the analysis of the thermal conductivity graph, there is an increase in thermal conductivity from the control condition (0 %) of 0.1610 $W \cdot m^{-1} \cdot K^{-1}$ to a nanoparticle concentration of $\Phi = 0.30$ %, which reaches 0.1620 $W \cdot m^{-1} \cdot K^{-1}$, an increase of approximately 1.24 %. This may be compared to the research conducted by Vora *et al.* (2023), where there was an increase in the value of thermal conductivity in nanofluid Al_2O_3/castor oil by 17.4 % at a concentration of 0.50 wt%. The range of values that are quite varied compared to this study is due to differences in several factors, such as the type of base fluid, type of nanoparticle and size, concentration, test temperature, and dispersion stability. Although the increase in this study is relatively small, it remains in the relevant category in MQL. This increase indicates a positive relationship between nanoparticle concentration and thermal conductivity: the higher the nanoparticle concentration (higher Φ), the greater the thermal conductivity (Manikandan & Nanthakumar, 2024). Although there is a small decrease at $\Phi = 0.15$ % (0.1607 $W \cdot m^{-1} \cdot K^{-1}$), which is common in nanofluids, overall, the thermal conductivity remains stable. This indicates that the addition of nanoparticles can increase thermal conductivity by expanding the surface area for heat transfer, although an increase in fluid viscosity also occurs (Kim *et al.*, 2015).

In general, the increase in thermal conductivity of nanofluids is influenced by several factors, namely: the concentration of nanoparticles, the type of nanoparticle material, and temperature (Bertolini *et al.*, 2021; Halelfadl *et al.*, 2013). Nanoparticles with high thermal conductivity will be more effective in increasing the thermal conductivity of nanofluids compared to nanoparticles that have low thermal conductivity (Jang *et al.*, 2022). In addition, the higher the concentration of nanoparticles in the fluid, the higher the thermal conductivity of the nanofluids. A moderate increase in thermal conductivity in GNP-rich CO nanofluids will be very beneficial for improving cooling capabilities in the machining process. With higher thermal conductivity, nanofluids can be more effective in transferring heat from the cutting zone, thereby reducing the cutting temperature and preventing tool wear more effectively.

3.2. Dynamic viscosity

The following are the results of the viscosity test of nanofluids against rotation at temperatures of 40 °C, 60 °C, 80 °C, and 100 °C (Fig. 6). The purpose of this test is to analyze the dynamic viscosity at various temperatures against the weight percentage of GNP. The results obtained in this study will provide the potential for GNP/CO fluid as a cutting fluid used in machining processes.

The decrease in viscosity at high shear rates provides advantages in the cooling process in machining. Cooling in the cutting zone increases the high shear rate. This condition allows fluid to flow more easily at the tool-workpiece interface, thereby minimizing temperature and tool wear. The highest viscosity is produced at a weight percentage of 0.20 % GNP at all temperatures, while the lowest is produced in pure CO. The addition of nanoparticles to the CO solution increases the GNP concentration, resulting in a higher dynamic viscosity value for the nanofluid. However, the increase in dynamic viscosity with increasing concentration is not always linear or significant, especially at higher concentrations or in systems with complex interparticle interactions (Yahya *et al.*, 2024). In addition, the increase in viscosity is also caused by the presence of van der Waals attraction forces, where the inhibition of non-particle agglomeration occurs due to electrostatic repulsion caused by the presence of surfactants. Increasing the concentration of GNP will make the attractive force become more dominant than the repulsive force, causing agglomeration in the nanoparticles (Ebrahim *et al.*, 2023). Agglomeration in nanoparticles requires a greater force to separate the dispersed particles so that the internal shear stress in the nanofluid increases. This condition will linearly increase the viscosity (Müller *et al.*, 2021). Dynamic viscosity in cutting fluid applications plays a very important role, especially in thermal characteristics. In addition, cutting fluid with the right viscosity will provide a high film layer in the machining process, thereby minimizing tool wear.

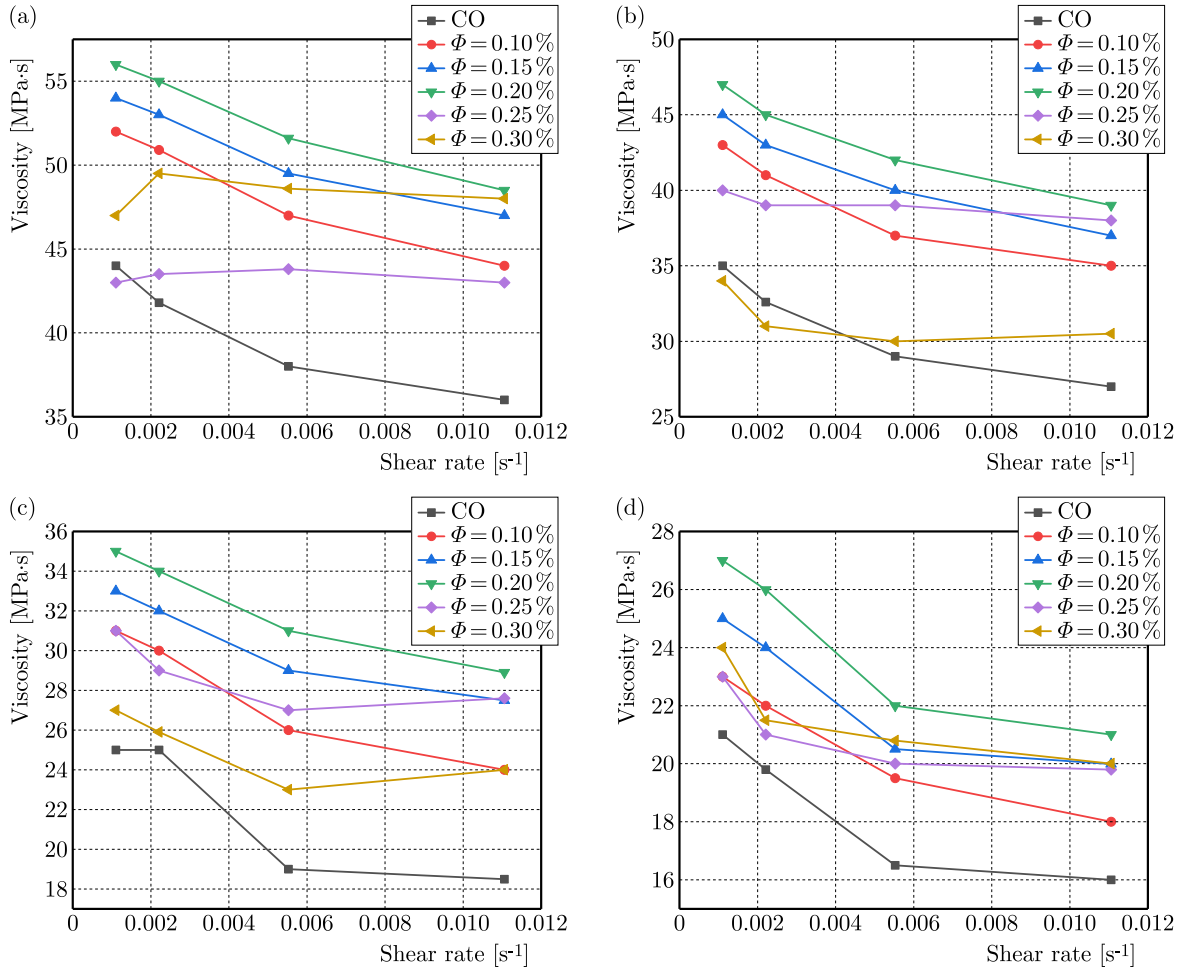

Fig. 6. Dynamic viscosity of cutting fluid versus shear rate at different temperatures: (a) 40 °C; (b) 60 °C; (c) 80 °C; (d) 100 °C. The case $\Phi = 0\,\%$ (corn oil (CO)) represents the base cutting fluid without GNPs, and legends indicate GNP concentrations ($\Phi = 0.10\,\%$ to $0.30\,\%$).

Viscosity decreases with an increasing shear rate (Fig. 6 and Fig. 7). This behavior exhibits pseudoplastic characteristics commonly found in nanofluids. In machining processes, this behavior is crucial because the contact area between the tool surface and the workpiece is very

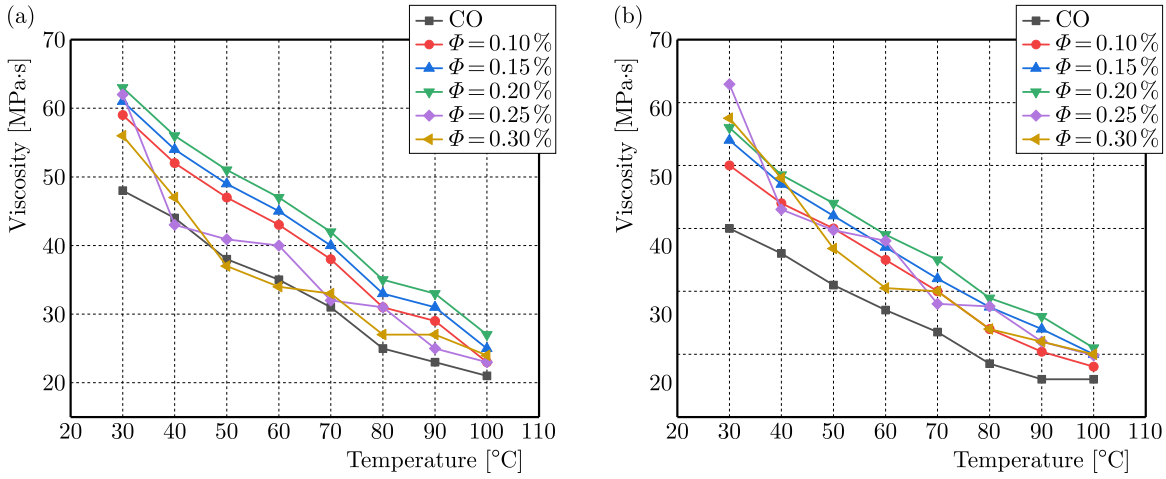

Fig. 7. Viscosity of cutting fluids with temperature at constant shear rates: (a) $0.0011\,\mathrm{s}^{-1}$ and (b) $0.011\,\mathrm{s}^{-1}$. The case $\Phi = 0\,\%$ (corn oil (CO)) represents the base cutting fluid without GNPs, and legends indicate GNP concentrations ($\Phi = 0.10\,\%$ to $0.30\,\%$).

large, causing the fluid to become thinner and accelerate flow in the cutting area, minimizing temperature and cooling efficiency. Conversely, under low shear rate conditions (before contact with the workpiece), the viscosity is relatively high, resulting in the formation of a strong film layer. The combination of high viscosity at low shear rates and low viscosity at high shear rates provides optimal protection and minimizes tool wear.

Under these conditions, in Fig. 7, the shear rate was kept constant between $0.0011\,s^{-1}$ and $0.011\,s^{-1}$, with a temperature range from 30 °C to 100 °C. The graph shows that viscosity decreases with increasing temperature at all shear rates. This decrease is caused by the increase in kinetic energy of fluid molecules at high temperatures, resulting in a weakening of intermolecular adhesion forces (La Mantia *et al.*, 2021). In general, Fig. 7 shows that viscosity decreases at high temperatures but remains stable up to 100 °C. This condition is also important in MQL cooling because high temperatures can reduce film thickness. However, because the viscosity decrease occurs in a controlled manner, the flow and distribution of the lubricant on the tool surface remain uniform.

3.3. Rheology

The results of the nanofluid rheology test can be seen in Fig. 8, which presents the relationship between shear stress and shear rates for GNP/CO nanofluid, showing that shear stress increases linearly with the shear rate at various temperatures. The Ostwald–de Waele method relates to the relationship between shear stress and the shear rate, which is used in calculating the

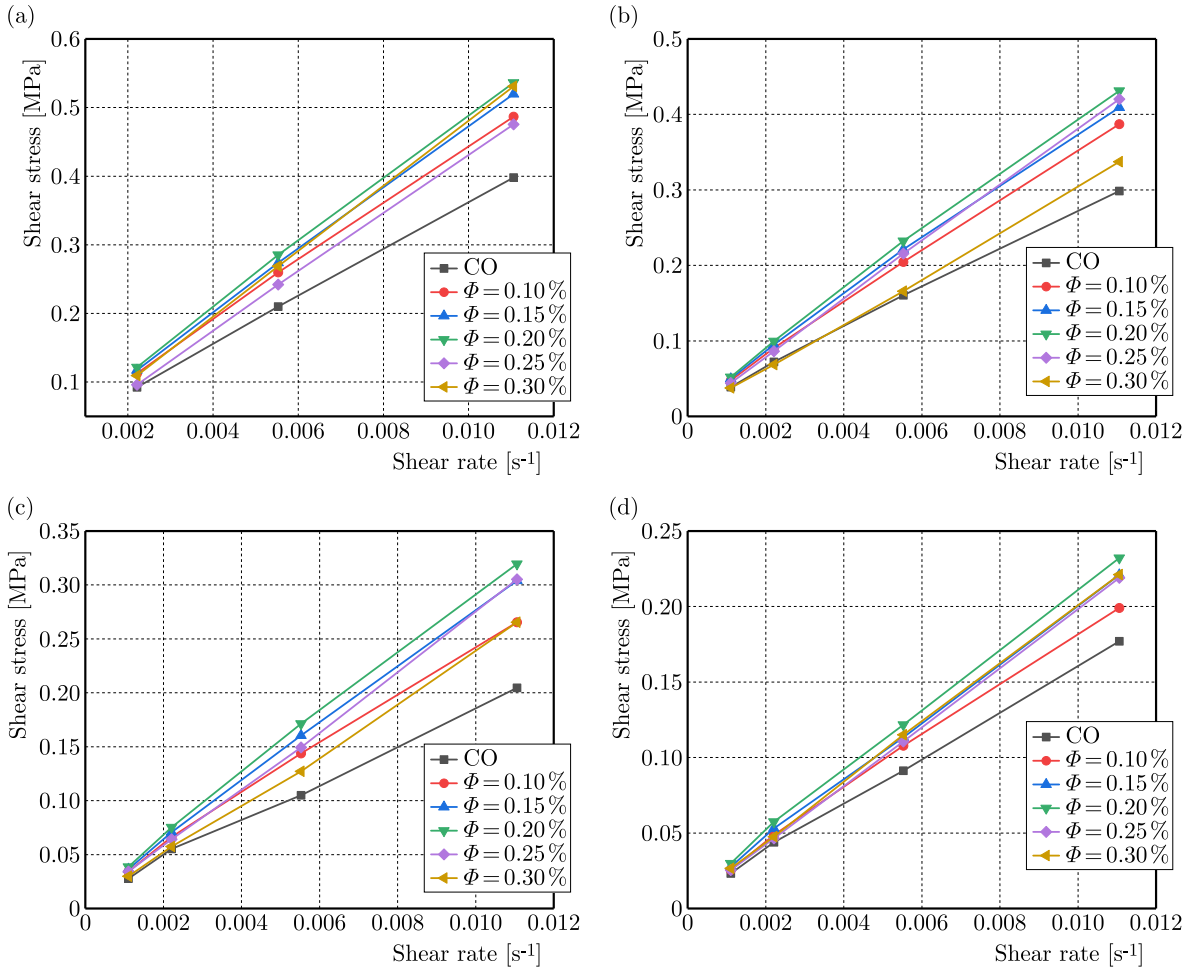

Fig. 8. Shear stress versus shear rate of cutting fluid at different temperatures: (a) 40 °C; (b) 60 °C; (c) 80 °C; (d) 100 °C. The case $\Phi = 0\,\%$ (corn oil (CO)) represents the base cutting fluid without GNPs, and legends indicate GNP concentrations ($\Phi = 0.10\,\%$ to $0.30\,\%$).

consistency index (m) and flow index (n). A flow index less than 1 indicates pseudoplastic behavior. Pseudoplastic behavior is characterized by a decrease in viscosity as the shear rate increases. Conversely, a flow index greater than 1 indicates dilatant flow, where an increase in the shear rate is followed linearly by viscosity (Chehadeh *et al.*, 2023).

At concentrations >0.20 wt%, the n value drops below 1 (e.g., 0.867 at 0.30 wt%), indicating a more dominant pseudoplastic behavior. This property is beneficial in increasing fluid penetration in the micro-contact area between the tool and the workpiece, where high friction and heat concentration occur.

Table 2 and Fig. 9 show that the power law index value at GNP percentage of 0.10 % to 0.20 % deviates from 1 (0.937–0.974). This value is still within the experimental uncertainty limit (±0.05), so it can be categorized as almost Newtonian, where the viscosity is relatively stable

Table 2. Power law index (n) and consistency index (m).

GNP [wt%]	Index	Temperature			
		40 °C	60 °C	80 °C	100 °C
0	m	26.588	17.422	25.000	11.783
	n	0.926	0.898	1	0.915
0.10	m	42.151	42.151	22.465	14.864
	n	0.969	0.969	0.953	0.936
0.15	m	44.944	28.795	8.995	16.743
	n	0.973	0.934	0.809	0.941
0.20	m	46.918	30.664	26.329	18.568
	n	0.974	0.937	0.958	0.945
0.25	m	48.170	31.194	16.103	9.413
	n	1.017	0.963	0.904	0.869
0.30	m	78.187	13.725	18.568	8.148
	n	1.075	0.867	0.945	0.841

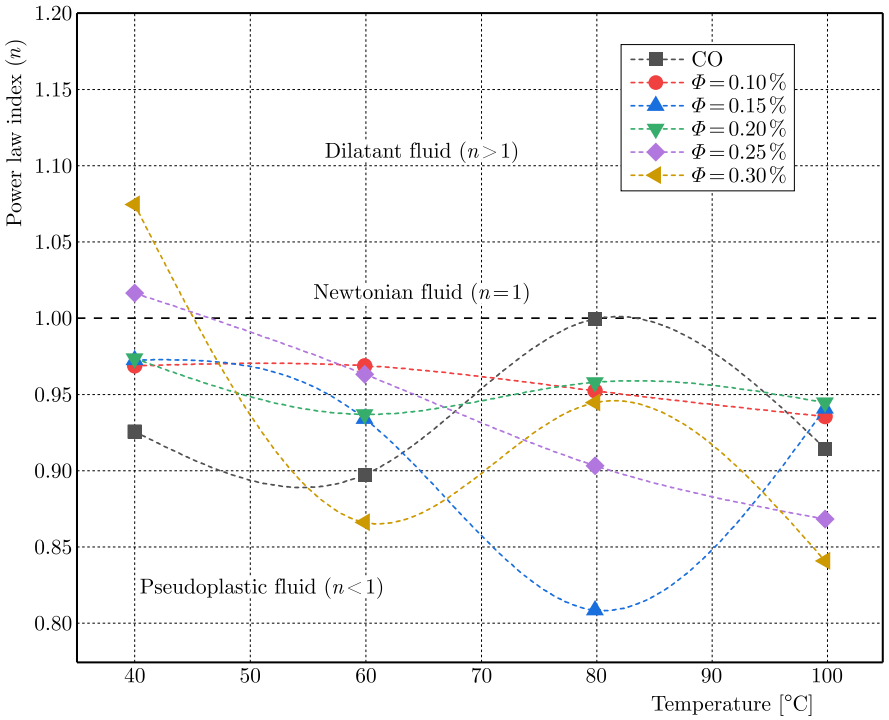

Fig. 9. Power law index against temperature for corn oil (CO, $\Phi = 0\,\%$) and nanoparticle-enhanced fluids with volume fractions $\Phi = 0.10\,\%$ to $0.30\,\%$.

against changes in the shear rate. This stability is crucial for low-pressure MQL lubrication systems because it ensures a constant flow from the nozzle into the cutting zone area, prevents spray fluctuations, and produces a uniform lubricant film (Gomez *et al.*, 2022).

Furthermore, Fig. 10 shows the relationship between the consistency index and temperature. The consistency index appears to decrease with increasing temperature. This condition indicates that with increasing temperature, fluid mobility also decreases and has an impact on reducing resistance in flowing fluid. Increasing temperature causes molecules in the fluid to move faster, reduces interactions between molecules as well as fluid viscosity. In addition, this generally occurs in pseudoplastic fluids (power law), where the dynamic viscosity value decreases exponentially with temperature, whereas according to the Arrhenius model, this is a normal effect based on increasing molecular energy and the release of internal structural networks (Adebowale & Sanni, 2013; Ahmed & Ramaswamy, 2003). Furthermore, the decrease in temperature under MQL conditions increases cooling efficiency because the fluid flows more easily and absorbs heat at high temperatures. However, this tendency needs to be optimized to avoid compromising the strength of the lubricant film at extreme temperatures.

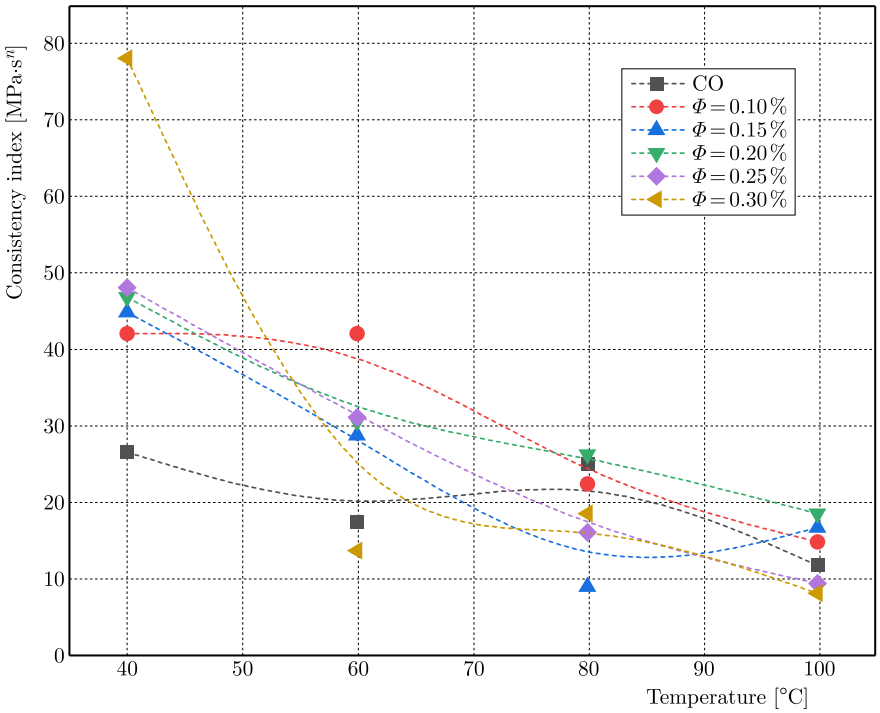

Fig. 10. Consistency index against temperature for corn oil (CO, $\Phi = 0\,\%$) and nanoparticle-enhanced fluids with volume fractions $\Phi = 0.10\,\%$ to $0.30\,\%$.

4. Conclusion

The purpose of this study was to analyze the thermal conductivity, dynamic viscosity, and rheological behavior of CO combined with GNPs. The results showed that the highest thermal conductivity was obtained at a concentration of $\Phi = 0.30\,\mathrm{wt\%}$, with a value of $0.1620\,\mathrm{W \cdot m^{-1} \cdot K^{-1}}$. This increase in thermal conductivity will provide the nanofluid's ability to remove heat from the cutting zone area, thereby reducing cutting temperatures and reducing tool wear. The highest viscosity value was found at $\Phi = 0.20\,\mathrm{wt\%}$, which indicates that increasing the GNP concentration strengthens the intermolecular attractive forces and encourages particle agglomeration. This agglomeration requires more energy to maintain dispersion stability, which can affect long-term performance. Rheological results show that nanofluids at $\Phi = 0.10\,\%$ and $\Phi = 0.20\,\%$ exhibit near-Newtonian properties, with a flow index (n) close to 1. This viscosity stability against changes in the shear rate is very beneficial in the lubrication of machining processes, as it en-

sures a constant fluid flow in the MQL nozzle and the formation of a uniform lubricant film at the tool-chip interface. Overall, GNP-CO nanofluid has the potential to be an environmentally friendly lubricant capable of improving cooling efficiency, reducing friction, and minimizing tool wear under real-world machining conditions. However, further research is needed to improve sedimentation stability and long-term dispersion resistance, which are important factors in industrial applications.

Acknowledgments

This research received funding support from the Ministry of Research and Technology (Directorate General of Higher Education) through a BPPDN scholarship under contract number B/67/D.D3/KD.02.00/2019. Furthermore, this research received funding support from the University of Merdeka Malang through the LPPM (Research Institute for Research and Community Service) in 2025. This research received data analysis and review support from Prof. Mahros Darsin, S.T., M.Sc., Ph.D., a lecturer at the University of Jember.

References

1. Adebowale, A.-R.A., & Sanni, L.O. (2013). Effects of solid content and temperature on viscosity of tapioca meal. *Journal of Food Science and Technology*, *50*(3), 573–578. https://doi.org/10.1007/s13197-011-0363-7
2. Ahmed, J., & Ramaswamy, H.S. (2003). Effect of high-hydrostatic pressure and temperature on rheological characteristics of glycomacropeptide. *Journal of Dairy Science*, *86*(5), 1535–1540. https://doi.org/10.3168/jds.S0022-0302(03)73738-2
3. Arsene, B., Gheorghe, C., Sarbu, F.A., Barbu, M., Cioca, L.-I., & Calefariu, G. (2021). MQL-assisted hard turning of AISI D2 steel with corn oil: Analysis of surface roughness, tool wear, and manufacturing costs. *Metals*, *11*(12), Article 2058. https://doi.org/10.3390/met11122058
4. Bertolini, R., Ghiotti, A., & Bruschi, S. (2021). Graphene nanoplatelets as additives to MQL for improving tool life in machining Inconel 718 alloy. *Wear*, *476*, Article 203656. https://doi.org/10.1016/j.wear.2021.203656
5. Caglayan, M.O. (2021). Rheological and tribological characterization of novel modified graphene/oil-based nanofluids using force microscopy. *Microscopy Research & Technique*, *84*(4), 814–827. https://doi.org/10.1002/jemt.23641
6. Chehadeh, D., Ma, X., & Al Bazzaz, H. (2023). Recent progress in hydrotreating kinetics and modeling of heavy oil and residue: A review. *Fuel*, *334*(1), Article 126404. https://doi.org/10.1016/j.fuel.2022.126404
7. Da Silva, R.B., Vieira, J.M., Cardoso, R.N., Carvalho, H.C., Costa, E.S., Machado, A.R., & De Ávila, R.F. (2011). Tool wear analysis in milling of medium carbon steel with coated cemented carbide inserts using different machining lubrication/cooling systems. *Wear*, *271*(9–10), 2459–2465. https://doi.org/10.1016/j.wear.2010.12.046
8. Debnath, S., Reddy, M.M., & Yi, Q.S. (2014). Environmental friendly cutting fluids and cooling techniques in machining: A review. *Journal of Cleaner Production*, *83*, 33–47. https://doi.org/10.1016/j.jclepro.2014.07.071
9. Ebrahim, S.A., Pradeep, E., Mukherjee, S., & Ali, N. (2023). Rheological behavior of dilute graphene-water nanofluids using various surfactants: An experimental evaluation. *Journal of Molecular Liquids*, *370*, Article 120987. https://doi.org/10.1016/j.molliq.2022.120987
10. Gómez-Merino, A.I., Jiménez-Galea, J.J., Rubio-Hernández, F.J., & Santos-Ráez, I.M. (2022). Experimental assessment of thermal and rheological properties of coconut oil-silica as green additives in drilling performance based on minimum quantity of cutting fluids. *Journal of Cleaner Production*, *368*, Article 133104. https://doi.org/10.1016/j.jclepro.2022.133104
11. Gunjal, S.U., & Patil, N.G. (2018). Experimental investigations into turning of hardened AISI 4340 steel using vegetable based cutting fluids under minimum quantity lubrication. *Procedia Manufacturing*, *20*, 18–23. https://doi.org/10.1016/j.promfg.2018.02.003

12. Halelfadl, S., Estellé, P., Aladag, B., Doner, N., & Maré, T. (2013). Viscosity of carbon nanotubes water-based nanofluids: Influence of concentration and temperature. *International Journal of Thermal Sciences*, *71*, 111–117. https://doi.org/10.1016/j.ijthermalsci.2013.04.013

13. Jang, J.-u., Nam, H.E., So, S.O., Lee, H., Kim, G.S., Kim, S.Y., & Kim, S.H. (2022). Thermal percolation behavior in thermal conductivity of polymer nanocomposite with lateral size of graphene nanoplatelet. *Polymers*, *14*(2), Article 323. https://doi.org/10.3390/polym14020323

14. Kim, S.Y., Noh, Y.J., & Yu, J. (2015). Thermal conductivity of graphene nanoplatelets filled composites fabricated by solvent-free processing for the excellent filler dispersion and a theoretical approach for the composites containing the geometrized fillers. *Composites Part A: Applied Science and Manufacturing*, *69*, 219–225. https://doi.org/10.1016/j.compositesa.2014.11.018

15. La Mantia, F.P., Titone, V., Milazzo, A., Ceraulo, M., & Botta, L. (2021). Morphology, rheological and mechanical properties of isotropic and anisotropic PP/rPET/GnP nanocomposite samples. *Nanomaterials*, *11*(11), Article 3058. https://doi.org/10.3390/nano11113058

16. Manikandan, S., & Nanthakumar, A.J.D. (2024). Development of a predictive model for thermal conductivity in graphene nanoplatelets-infused damper oil using ANN/RSM. *Thermal Science*, *28*(5B), 4235–4247. https://doi.org/10.2298/TSCI231130152M

17. Manikanta, J.E., Naga Raju, B., & Satankar, R.K. (2024). Development and characterization of novel green cutting fluids with nano-additives. *Periodica Polytechnica Mechanical Engineering*, *68*(4), 304–311. https://doi.org/10.3311/PPme.23466

18. Müller, M., Stahl, L., Arafat, R., Madanchi, N., & Herrmann, C. (2021). A case study on the observability of cutting fluid flow and the associated contact mechanics in scaled rough surfaces. *SN Applied Sciences*, *3*(5), Article 570. https://doi.org/10.1007/s42452-021-04572-x

19. Park, K.-H., Ewald, B. & Kwon, P.Y. (2011). Effect of nano-enhanced lubricant in minimum quantity lubrication balling milling. *Journal of Tribology*, *133*(3), Article 031803. https://doi.org/10.1115/1.4004339

20. Ramón-Raygoza, E.D., Rivera-Solorio, C.I., Giménez-Torres, E., Maldonado-Cortés, D., Cardenas-Alemán, E., & Cué-Sampedro, R. (2016). Development of nanolubricant based on impregnated multilayer graphene for automotive applications: Analysis of tribological properties. *Powder Technology*, *302*, 363–371. https://doi.org/10.1016/j.powtec.2016.08.072

21. Samuel, J., Rafiee, J., Dhiman, P., Yu, Z.-Z., & Koratkar, N. (2011). Graphene colloidal suspensions as high performance semi-synthetic metal-working fluids. *The Journal of Physical Chemistry C*, *115*(8), 3410–3415. https://doi.org/10.1021/jp110885n

22. Uysal, A. (2017). An experimental study on cutting temperature and burr in milling of ferritic stainless steel under MQL using nano graphene reinforced cutting fluid. *Advanced Materials Proceedings*, *2*(9), 560–563. https://doi.org/10.5185/amp.2017/038

23. Vora, V., Sharma, R.K., & Bharambe, D.P. (2023). Investigation of rheological and thermal conductivity properties of castor oil nanofluids containing graphene nanoplatelets. *International Journal of Thermophysics*, *44*(10), Article 155. https://doi.org/10.1007/s10765-023-03264-5

24. Wang, B., Yang, Q., Deng, J., Hou, N., Wang, X., & Wang, M. (2022). Effect of graphene nanoparticles and sulfurized additives to MQL for the machining of Ti-6Al-4 V. *The International Journal of Advanced Manufacturing Technology*, *119*(5–6), 2911–2921. https://doi.org/10.1007/s00170-021-08348-w

25. Yahya, M.N., Mohd Norddin, M.N.A., Ismail, I., Rasol, A.A.A., Risal, A.R., Yakasai, F., Oseh, J.O., Ngouangna, E.N., Younas, R., Ridzuan, N., Mahat, S.Q.A., & Agi, A. (2024). Graphene nanoplatelet surface modification for rheological properties enhancement in drilling fluid operations: A review. *Arabian Journal for Science and Engineering*, *49*(6), 7751–7781. https://doi.org/10.1007/s13369-023-08458-5

Manuscript received August 8, 2025; accepted for publication November 21, 2025; published online February 13, 2026.